Published in final edited form as:
J Pharmacokinet Pharmacodyn. 2014 December ; 41(6): 571–580. doi:10.1007/s10928-014-9374-0.

Survey of monoclonal antibody disposition in man utilizing a minimal physiologically-based pharmacokinetic model

Yanguang Cao and **William J Jusko**
Department of Pharmaceutical Sciences, School of Pharmacy and Pharmaceutical Sciences, State University of New York at Buffalo, Buffalo, NY, 14214, USA

William J Jusko: wjjusko@buffalo.edu

Abstract

Minimal physiologically based pharmacokinetic (mPBPK) models provide a simple and sensible approach that incorporates physiological elements into pharmacokinetic (PK) analysis when only plasma data are available. With this modeling concept, a second-generation mPBPK model was further developed with specific accommodations for the unique PK properties of monoclonal antibodies (mAb). This study applied this model to extensively survey mAb PK in man in order to seek general perspectives on mAb distributional and elimination features. Profiles for 72 antibodies were successfully analyzed with this model. The model results provide assessment regarding: 1) predominant clearance site, in plasma or interstitial fluid (*ISF*); 2) mAb *ISF* concentrations in two groups of lumped tissues with continuous (V_{tight}) or fenestrated (V_{leaky}) vascular endothelium; 3) Transcapillary Escape Rate (*TER*), an indicator of systemic vascular permeability. For 93% of surveyed mAbs, the model assuming clearance from plasma (CL_p) produced better or at least equivalent model performance than the model with clearance from *ISF* and yielded most consistent values of vascular reflection coefficients (σ_1 and σ_2) among all antibodies. The average mAb *ISF* concentration in V_{tight} and V_{leaky} at equilibrium was predicted to be about 6.8% and 37.9% of that in plasma. A positive correlation was detected between plasma clearance and *TER* among most mAbs, which could be interpreted as both parameters having common determinants related to *ISF* tissue distribution in this model context. The mAbs with relative higher plasma clearance (> 0.035 L/hr/70 kg) did not reveal such positive correlation between clearance and *TER*, implying that the factors contributing to high clearance may not necessarily increase tissue distribution and penetration. In conclusion, this mPBPK model offers a more mechanistic approach for analyzing plasma mAb PK than compartment models and generates parameters providing useful intrinsic distributional and elimination insights for a large number of mAbs that were examined in man.

Keywords

PBPK; minimal PBPK models; monoclonal antibody; distribution

Introduction

Over the last three decades, monoclonal antibodies (mAb) have dramatically transformed drug discovery and human therapeutics. More than 30 antibodies have been approved by the U.S. Food and Drug Administration, and hundreds of candidates are in clinical trials [1]. So

far, most of the approved mAbs are used for cancer [2] and autoimmune diseases [3], but it is likely that therapeutic antibodies will find indications for a variety of other diseases.

Pharmacokinetic (PK) studies are important in almost every stage of drug development and a proper PK model can assist in quantitation and prediction of drug properties [4]. It has been well documented that mAbs exhibit many different PK behaviors from small molecules [5], such as limited vascular permeability, much less renal filtration and hepatic metabolism, and more common receptor-mediated nonlinearity. Models that specially accommodate these PK features would be helpful. Although a typical bi-exponential PK profile is often observed for many mAbs, the underlying processes are intrinsically different from small molecules. Hence, in mAb PK analysis, classical PK approaches (noncompartmental analysis (NCA), twocompartment models (2CM)) should be applied with caution as the analysis results sometimes involve problems for interpretation [6, 7], particularly for those mAbs with activity within or clearance from peripheral tissues that are not in rapid equilibrium with plasma.

Minimal physiologically-based pharmacokinetic (mPBPK) models offer a simple and sensible modeling approach to incorporate physiological elements into pharmacokinetic (PK) analysis when only plasma data are available [8]. We introduced a second-generation mPBPK model, which was developed in specific consideration of those unique PK behaviors of mAb [9]. Specifically, the model divides the system tissues into two groups based on the structure of their vascular endothelium, continuous and discontinuous or fenestrated. Lymph was separately considered in this model and convection was assumed as the primary distribution and recycling mechanism. This model has shown the potential to serve as a general approach if one can only analyze mAb plasma concentration vs time data and it generates parameters providing better PK insights than NCA and the 2CM mammillary model. One feature of this model is predicting antibody concentrations in the *ISF* of two groups of lumped tissues, which is always a challenging task for experimental measurements. This becomes particularly important for antibodies with targets in *ISF*, as the predicted *ISF* concentrations may allow assessments of receptor occupancy and the following pharmacodynamics at the site of action, which otherwise has to rely on plasma concentrations.

The study applies this model to over 80 literature-surveyed mAb PK profiles in man, mainly to: 1) evaluate the feasibility of this model as a general modeling approach for mAb PK analysis; and 2) seek general perspectives of distributional and elimination properties of available mAbs.

Theoretical

Second-generation mPBPK model

The second-generation mPBPK model was developed specifically for linear mAb PK analysis (9). The model structure is shown in Figure 1. Two groups of tissues (V_{tight} and V_{leaky}) were defined in the model according to the vascular endothelial structure as *ISF* volumes in tissues that have continuous or fenestrated capillaries [10]. The V_{tight} includes muscle, skin, adipose and brain and V_{leaky} refers to all other tissues (liver, kidney, heart,

etc). Model A assumed clearance from plasma and Model B assumed clearance from *ISF*. The differential equations for the model A (with CL_p) are:

$$\frac{dC_p}{\mathrm{dt}}=\frac{Input}{V_p}+[C_{lymph}\bullet L-C_p\bullet L_1\bullet(1-\sigma_1)-C_p\bullet L_2\bullet(1-\sigma_2)-C_p\bullet CL_p]/V_p \quad (1)$$

$$\frac{dC_{tight}}{\mathrm{dt}}=[L_1\bullet(1-\sigma_1)\bullet C_p-L_1\bullet(1-\sigma_L)\bullet C_{tight}]/V_{tight} \quad (2)$$

$$\frac{dC_{leaky}}{\mathrm{dt}}=[L_2\bullet(1-\sigma_2)\bullet C_p-L_2\bullet(1-\sigma_L)\bullet C_{leaky}]/V_{leaky} \quad (3)$$

$$\frac{dC_{lymph}}{\mathrm{dt}}=[L_1\bullet(1-\sigma_L)\bullet C_{tight}+L_2\bullet(1-\sigma_L)\bullet C_{leaky}-C_{lymph}\bullet L]/V_{\mathrm{lymph}} \quad (4)$$

where C_p and C_{lymph} are antibody concentrations in plasma and lymph and C_{tight} and C_{leaky} are antibody concentrations in tissues with continuous endothelium (V_{tight}) and with fenestrated or discontinuous endothelium (V_{leaky}). The L is total lymph flow and equals the sum of L_1 and L_2, where $L_1 = 0.33\bullet L$ and $L_2 = 0.67\bullet L$. These fractions were derived from previously used values of lymph flow in full PBPK models [11, 12] except for brain that has no measurable lymph flow [13]. The σ_1 and σ_2 are vascular reflection coefficients for V_{tight} and V_{leaky}. The σ_L is the lymphatic capillary reflection coefficient, which is assumed to be 0.2 [11]. The CL_i and CL_p are clearances from *ISF* and plasma. All Initial Conditions are concentrations = 0.

The physiological restrictions are: V_p is plasma volume and V_{lymph} is total lymph volume, and:

$$\sigma_1<1 \text{ and } \sigma_2<1 \quad (5a, b)$$

$$V_{tight}=0.65\cdot ISF\cdot K_p \text{ and } V_{leaky}=0.35\cdot ISF\cdot K_p \quad (6a, b)$$

where *ISF* is total system *ISF* and K_p is available fraction of *ISF* for antibody distribution. The physiologic parameters [14, 15] for a 70 kg body weight person are: L = 2.9 L/day, *ISF* = 15.6 L, V_{lymph} = 5.2 L, and V_{plasma} = 2.6 L. Also, K_p = 0.8 for native IgG_1 and 0.4 for native IgG_4 [16, 17].

Only three parameters need to be estimated in this model: σ_1, σ_2 and CL_p (or CL_i). The two clearances are not estimated together, but the model can test which one works better. One point should be clarified is that this model does not enact the function of FcRn according to our previous analysis [9]. The analysis showed that FcRn may play important role in antibody systemic persistence but may not substantially contribute to tissue distribution.

The Transcapillary Escape Rate (*TER*) is the sum of two routes,

$$TER = L_1 \bullet (1 - \sigma_1) + L_2 \bullet (1 - \sigma_2) \quad (7)$$

The concentration ratios at equilibrium between *ISF* and plasma can be calculated in Model A as,

$$(1 - \sigma_1)/(1 - \sigma_L) \text{for} V_{tight} \text{ and } (1 - \sigma_2)/(1 - \sigma_L) \text{for} V_{leaky} \quad (8a, b)$$

In Model B, where clearance from *ISF* (CL_i) is assumed, the ratios are:

$$\frac{C_{Tight}}{C_p} = \frac{L_1 \bullet (1 - \sigma_1)}{L_1 \bullet (1 - \sigma_L) + CL_i} \text{ and } \frac{C_{Leaky}}{C_p} = \frac{L_2 \bullet (1 - \sigma_2)}{L_2 \bullet (1 - \sigma_L) + CL_i} \quad (9a, b)$$

As shown in Eq. (7) – (9), the vascular reflection coefficients (σ_1 and σ_2) are parameters that not only determine transcapillary rate but also predict the extent of distribution. The lower vascular reflection coefficient produces a more rapid transcapillary rate, resulting in earlier peaking and higher concentrations of mAb in the lumped *ISF* compartment.

The ADAPT and WinNonlin model codes for these equations were provided previously [9].

Data analysis

The second-generation mPBPK model was applied to analyze 83 mAb PK profiles found in the literature for man (Tables 1 and 2). The mAbs selected were those with linear PK in the tested dose range and study conditions. Plasma concentration versus time data for these antibodies were captured using Digitizer software. Where possible, a wide range of doses were utilized with all data for each mAb and fitted jointly. Given the similar isoelectric point (p*I*) values (in the range of 8-9) of the currently assessed mAbs with native IgG_1, K_p was set to 0.8 in this analysis.

Two clearance mechanisms CL_i and CL_p were tested and compared in terms of model performance and parameter estimates. Three categories were defined to indicate the preference for Model A with CL_p for the overall clearance: “Yes”, “Similar”, and “No”. Based on the results obtained from the model with CL_p, “Yes” was defined by either better model performance in comparison with the model with CL_i (ΔObj < - 3.0), or the model with CL_i resulted in unreasonable estimated parameters, such as $\sigma_1 < \sigma_2$ or with minute σ values; “Similar” was defined by comparable model performance with reasonable parameter estimates; “No” was defined by poorer model performance (ΔObj > 3.0) than the model with CL_i and less reasonable parameter estimates.

All fittings utilized the maximum likelihood method in ADAPT 5 [18] and naïve pooled data modeling. The variance model was:

$$V_i = (intercept + slope \cdot Y(t_i))^2 \quad (10)$$

where: V_i is the variance of the response at the ith time point, t_i is the actual time at the ith time point, and $Y(t_i)$ is the predicted response at time t_i from the model. Variance parameter *intercept* and *slope* were estimated together with system parameters.

Model performance was evaluated by goodness-of-fittings, visual inspection, sum of square residuals, Akaike Information Criterion (*AIC*), Schwarz Criterion (*SC*), and Coefficient of Variation (*CV*) of the estimated parameters.

Results

The second-generation mPBPK model provides a modeling approach specifically for PK analysis of mAbs. The model, with several assumed physiologic parameters and fitting only plasma concentration vs time data, provides estimations of average vascular reflection coefficients (σ_1 and σ_2) and assesses the possible location of predominant clearance in either plasma or *ISF*. Values of *TER* were calculated from the estimated σ_1 and σ_2 values (Eq. (7)) to reflect the overall vascular permeability. The equilibrium concentration ratio (*ISF* / *Plasma*) was predicted based on the estimated σ (Eq. (8)) and clearance values (Eq. (9)). Literature data for 83 mAbs with linear PK were analyzed with this modeling approach. Of these mAbs, 72 mAb PK profiles were well-captured with reasonable parameter estimates (Table 1). Representative plasma concentration versus time profiles are shown for 9 mAbs in Figure 2. Additional fitted mAb profiles were shown in our previous publication [9]. Eleven mAbs failed with this model due to several speculative reasons (Table 2).

Single or several dose profiles were characterized (Figure 2) and all parameters were estimated with reasonable precision (CV% < 50%) for the 72 well-captured mAbs (Table 1). In the model with CL_p, the estimated σ_1 ranged from 0.693 to 0.999 with an average of 0.945 and σ_2 ranged from 0.202 to 0.984 with an average of 0.697. The grouped σ_1 values showed lower inter-antibody variability (CV% = 3.67%) than σ_2 (CV% =16.9%) (Figure 3). Some mAbs did not have sufficient data to support a clear identification of σ_1 different from 1, which resulted in an estimate of σ_1 as 1 (the physiological limit). In those cases, σ_1 was fixed to 0.95, the average value from the other mAbs with precise estimates of σ_1. No correlation ($r^2 = 0.038$) was found between σ_1 and σ_2 for the surveyed mAbs. The estimated values of CL_p ranged 0.517 – 66.4 mL/hr/70 kg with high inter-antibody variability (Figure 3). The average CL_p was 17.6 ± 15.0 mL/hr/70 kg. Of note, 9 mAbs (13%) showed relatively high clearance (> 35 mL/hr/70 kg).

Surprisingly, 11 mAbs failed in application of this model with either inadequately captured PK profiles or unreasonable parameter estimates. Table 2 lists these mAbs and provides the possible reasons. Figure 4 displays two representative suboptimal cases. For most of these mAbs, the mPBPK model had difficulties in capturing the initial phase (early α-phase). Given the fact that the mPBPK model assumes actual plasma volume as the initial distribution space, the under-prediction of the initial phase with such model assumption is unexpected and may be caused either by measurement error or blood collection from the infusion tubing in the original study. The over-prediction was speculated due to appreciable nonspecific binding of mAb in blood, a mechanism not included in the mPBPK model.

As indicated in Eq (8), the vascular reflection coefficients affect not only *TER* but also *ISF* concentrations. High *TER* values anticipate high *ISF* concentrations. Figure 5 displays the *ISF* / *Plasma* concentration ratios for V_{leaky} and V_{tight} that were calculated for all 72 mAbs listed in Table 1. The average ratios for V_{tight} were about 6.8% and for V_{leaky} about 37.9%. Six antibodies (tocilizumab, APG101, daclizumab, siplizumab, AMG386, aflibercept) had equilibrium ratios in V_{leaky} higher than 81%, indicating relatively high vascular permeability and probably rapid distribution of these mAbs into tissues with leaky endothelium.

Comparisons of Clearances

Table 1 lists the occurrence of model-based preference for a predominant CL_p that was implied by this modeling approach: 37 mAbs (51%) are “Yes”, 5 mAbs (7%) are “No”, and 30 mAbs (42%) are “Similar”. In the “Yes” group, the model with CL_p showed better model performance for 6 mAbs and the model with CL_i resulted in unreasonable parameter estimates (either $\sigma_1 < \sigma_2$ or very small σ) for the remaining 31 mAbs. In the “No” group, the model with CL_p showed worse model performance in comparison with model with CL_i. There are 30 mAbs in the “Similar” group that showed similar model performance and both models gave reasonable parameter estimates. Thus, for 93% of the well-fitted antibody PK profiles, the model with CL_p is either preferred or equivalent to that with CL_i.

Interestingly, as shown in Figure 6, many of the mAbs in the “Yes” group appeared to have higher clearances than the mAbs in the “Similar” group ($p = 0.035$), which suggests that the mAbs with relatively high clearance are more likely degraded or eliminated from plasma rather than from *ISF*. No statistical difference in clearances was detected between the mAbs in the “Yes” group and “No” group, probably because of the limited numbers in the latter group.

Distribution (TER) vs CL_p

The estimated *TER* values were in the range of 1.70 – 66.6 mL/hr/70 kg. As shown in Figure 7, the estimated *TER* is about 2.5-fold higher than CL_p values and *TER* positively correlated with CL_p ($r^2 = 0.336$). As mentioned before, higher *TER* generally produces higher *ISF* concentrations in this modeling context. Thus, such correlation also reflects a relationship between *ISF* distribution extent and CL_p. This provides further evidence in support of previous observations that enhancement of tissue distribution usually results in an increase in systemic clearance [19]. The mAbs with the highest clearances were not included in the regression and correlation analysis. No statistical difference was detected in comparison of the *TER* values for the high CL_p mAbs versus other mAbs (0.032 *vs* 0.026, $p = 0.28$). HuMv833 and gemtuzumab ozogamicin were mAbs as exceptions with fast clearance but relatively small *TER*.

As shown in Figure 7, the type of immunoglobulin did not appear to affect the *TER* or CL_p values, as the values for mAbs that were IgG_2 or IgG_4 were dispersed within the data for IgG1 mAbs.

Discussion

The mPBPK model provides a consistent and mechanistic approach for analyzing PK profiles for mAb and allows systematic comparisons of their elimination and distributional properties. By fitting only plasma data, the mPBPK model provides assessments regarding: 1) predominant clearance site, plasma or *ISF*; 2) *ISF* concentrations in two groups of lumped tissues, V_{leaky} and V_{tight}; 3) *TER*, an indicator of systemic vascular permeability. Many of these issues could not be easily addressed experimentally, but sometimes are essential for therapeutic mAb development and optimization. Therefore, the mPBPK model appears to be preferable for mAb PK analysis than the commonly used 2CM to address these critical issues when fitting only plasma data.

This survey indicated that an assumption of CL_p provides better or at least equal model performance than does CL_i for 93% of the surveyed mAbs. It can be seen in Table 1 that Model A with CL_p produces highly consistent values of σ_1 and σ_2 while Model B produces highly variable results. This may further suggest that CL_p reflects the most common nonspecific clearance mechanism for most mAbs. As stated in our previous analysis [9], the linear clearance in this model context mostly represents the nonspecific clearance and such a clearance preference may be not directly associated with target location. From a mechanistic perspective, the degradation in endothelial lysosomes contributes to CL_p in this model framework given the efficient endocytosis that allows rapid uptake of mAb into endothelial endosomes and the rapid ‘equilibrium’ between endothelial endosomes and plasma [20]. Although the functioning of FcRn was not enacted in this model, a higher FcRn affinity would reduce mAb lysosome degradation and anticipate a lower estimate of CL_p (data not shown). Then, for mAbs with a dominant CL_p, it may be of pharmacokinetic and therapeutic value to design features to increase systemic persistence via an improved FcRn-binding affinity. If CL_i is dominant, less efficiency is expected by this strategy. The present model allows assessment of the two clearance mechanisms and may help new mAb development strategy in this regard.

It should be clarified that a preference for CL_i or CL_p suggested by the model does not necessarily exclude the existence of the other. Both CL_i and CL_p processes could more or less exist. The use of model fitting for such discrimination should be followed by direct experimental validation, if possible, when this is an important issue. As shown in Table 2, modeling alone is often inadequate to differentiate the two clearance mechanisms.

Interestingly, the mAbs that were associated with a preferred CL_p tend to have higher clearance than the others (Figure 6). This could be related to their limited vascular permeability. Simulations of PK profiles with high values of CL_i provide a further explanation for this, as the plasma profiles and apparent plasma clearance would not further change when CL_i was set higher than *TER*. This is because the apparent plasma clearance would not go any higher than *TER* if the predominant clearance occurs in *ISF*. It is a similar principle to the well-stirred hepatic clearance model where the apparent plasma clearance would be largely restricted by blood flow and become less dependent on intrinsic clearance when intrinsic clearance is much higher than blood flow. Therefore, it is expected that, when a mAb has a high apparent plasma clearance, particularly a clearance higher than

distribution clearance (*TER*), it would become less likely to have a predominant CL_i. This also explains why the mAbs with high clearances (> 35 mL/hr/70 kg) were more often associated with a model-preferred CL_p (Table 1).

Many factors have been found to influence mAb tissue distribution and systemic clearance [21], including size, shape, hydrophobicity, and charge. The mPBPK model supports a positive correlation between tissue distribution and systemic clearance (Figure 7), but the isotype of the immunoglobulins was not a factor. The *TER* vs CL_p correlation poses a challenge in selection of strategies for improving tissue distribution to enhance target site exposure as the systemic clearance would probably increase consequently and offset the improved distribution. An increase of net positive charge has shown to increase both tissue retention and systemic clearance [19]. The effect of molecular size was also investigated in this scenario showing that a larger molecule would generally result in lower tissue penetration with reduced systemic clearance [22]. An optimum probably exists when putting all these factors together to consider a general balance between distribution and clearance. Whatever factors contribute to this, this positive correlation seems not applicable to mAbs with high clearances (> 35 mL/hr/70 kg), implying that the factors contributing to high clearance may not necessarily increase tissue distribution and penetration, in contrast with most mAbs and other macromolecules.

Our results and conclusions should be considered with some caution. Firstly, the fitting results for each mAb (Table 1) should be interpreted within the specific study conditions where the data were originally collected. For instance, some mAbs, such as rituximab [23] and cetuximab [24], display nonlinear PK in certain populations while our assessment only considered the subjects and dose ranges with linear PK. Secondly, the model did not take account of immunogenicity, differing measurement assays and variability, and concomitant medications. These factors could potentially impact mAb PK and result in different model fittings and parameter estimates. In addition, the data digitization and model fittings utilized the available average PK profiles and thus the parameter estimates are approximate. Other cautions relate to the model assumptions regarding the available fraction of *ISF* for mAb distribution, convection as the major extravasation mechanism, assuming the same CL_i in V_{leaky} and V_{tight}, and use of standard physiological constants. However, our assumptions allowed a simple and consistent starting point and allowed a global comparison among studies.

The present modeling approach can be useful in generally assessing mAb PK and in drug development. While further examination of structural features contributing to the variability in *TER* and CL_p values seen in Figure 7 is warranted, application of this model will provide an indication of whether the properties of a new mAb resemble most others, particularly for a related indication. Inconsistencies such as we noted in Table 2 may warrant more careful analytical or clinical evaluation. The model provides approximate *ISF* concentrations and can be readily extended to handle target-mediated drug disposition and dynamics [25]. If utilized for population analysis, physiologic features can be more easily incorporated for model components.

In conclusion, this study successfully applied the mPBPK model to extensively survey literature available mAb PK in man and clearly demonstrated the feasibility of this model as a general approach in mAb PK analysis. The estimated parameters reflect many intrinsic distributional and elimination insights and relations. Although the reductionist feature of the mPBPK model was emphasized in our previous publications [8, 9], specific considerations of other kinetic mechanisms, such as target-mediated drug disposition [25], formation of anti-drug antibodies, and target kinetics are also feasible in this modeling framework. This mPBPK model offers a more mechanistic approach using the major structural features of full PBPK models for mAbs in specifically analyzing mAb PK than found in compartment models and provides an intermediary method if a full PBPK model is not available.

Supplementary Material

Refer to Web version on PubMed Central for supplementary material.

Acknowledgments

This research was supported by the National Institutes of Health Grant GM57980 and the UB Center for Protein Therapeutics.

References

1. Reichert JM. Marketed therapeutic antibodies compendium. MAbs. 2012; 4:413–415. [PubMed: 22531442]
2. Sliwkowski MX, Mellman I. Antibody therapeutics in cancer. Science. 2013; 341:1192–1198. [PubMed: 24031011]
3. Chan AC, Carter PJ. Therapeutic antibodies for autoimmunity and inflammation. Nat Rev Immunol. 2010; 10:301–316. [PubMed: 20414204]
4. Lin JH, Lu AY. Role of pharmacokinetics and metabolism in drug discovery and development. Pharmacol Rev. 1997; 49:403–449. [PubMed: 9443165]
5. Wang W, Wang EQ, Balthasar JP. Monoclonal antibody pharmacokinetics and pharmacodynamics. Clin Pharmacol Ther. 2008; 84:548–558. [PubMed: 18784655]
6. Richter WF, Grimm HP, Theil FP. Potential errors in the volume of distribution estimation of therapeutic proteins composed of differently cleared components. J Pharmacokinet Pharmacodyn. 2011; 38:581–593. [PubMed: 21779940]
7. Garzone PD, Atkinson AJ Jr. In search of physiologically based distribution volume estimates for macromolecules. Clin Pharmacol Ther. 2012; 92:419–421. [PubMed: 22992670]
8. Cao Y, Jusko WJ. Applications of minimal physiologically-based pharmacokinetic models. J Pharmacokinet Pharmacodyn. 2012; 39:711–723. [PubMed: 23179857]
9. Cao Y, Balthasar JP, Jusko WJ. Second-generation minimal physiologically-based pharmacokinetic model for monoclonal antibodies. J Pharmacokinet Pharmacodyn. 2013; 40:597–607. [PubMed: 23996115]
10. Sarin H. Physiologic upper limits of pore size of different blood capillary types and another perspective on the dual pore theory of microvascular permeability. J Angiogenes Res. 2010; 2:14. [PubMed: 20701757]
11. Garg A, Balthasar JP. Physiologically-based pharmacokinetic (PBPK) model to predict IgG tissue kinetics in wild-type and FcRn-knockout mice. J Pharmacokinet Pharmacodyn. 2007; 34:687–709. [PubMed: 17636457]
12. Shah DK, Betts AM. Towards a platform PBPK model to characterize the plasma and tissue disposition of monoclonal antibodies in preclinical species and human. J Pharmacokinet Pharmacodyn. 2012; 39:67–86. [PubMed: 22143261]

13. Wagshul ME, Johnston M. The brain and the lymphatic system. Immunology of the Lymphatic System. 2013:143–164.

14. Davies B, Morris T. Physiological parameters in laboratory animals and humans. Pharm Res. 1993; 10:1093–1095. [PubMed: 8378254]

15. Stucker O, Pons-Himbert C, Laemmel E. Towards a better understanding of lymph circulation. Phlebolymphology. 2008; 15:31–36.

16. Wiig H, Tenstad O. Interstitial exclusion of positively and negatively charged IgG in rat skin and muscle. Am J Physiol Heart Circ Physiol. 2001; 280:H1505–1512. [PubMed: 11247760]

17. Wiig H, Kaysen GA, al-Bander HA, De Carlo M, Sibley L, Renkin EM. Interstitial exclusion of IgG in rat tissues estimated by continuous infusion. Am J Physiol. 1994; 266:H212–219. [PubMed: 8304502]

18. D'Argenio, DZ.; Schumitzky, A. ADAPT V User's Guide: Pharmacokinetic/Pharmacodynamic System Analysis Software Biomedical Simulations Resource. Los Angeles CA: 2009.

19. Boswell CA, Tesar DB, Mukhyala K, Theil FP, Fielder PJ, Khawli LA. Effects of charge on antibody tissue distribution and pharmacokinetics. Bioconjug Chem. 2010; 21:2153–2163. [PubMed: 21053952]

20. Davies PF, Ross R. Mediation of pinocytosis in cultured arterial smooth muscle and endothelial cells by platelet-derived growth factor. J Cell Biol. 1978; 79:663–671. [PubMed: 103882]

21. Bumbaca D, Boswell CA, Fielder PJ, Khawli LA. Physiochemical and biochemical factors influencing the pharmacokinetics of antibody therapeutics. AAPS J. 2012; 14:554–558. [PubMed: 22610647]

22. Schmidt MM, Wittrup KD. A modeling analysis of the effects of molecular size and binding affinity on tumor targeting. Mol Cancer Ther. 2009; 8:2861–2871. [PubMed: 19825804]

23. Golay J, Semenzato G, Rambaldi A, Foa R, Gaidano G, Gamba E, Pane F, Pinto A, Specchia G, Zaja F, Regazzi M. Lessons for the clinic from rituximab pharmacokinetics and pharmacodynamics. MAbs. 2013; 5:826–837. [PubMed: 23933992]

24. Tan AR, Moore DF, Hidalgo M, Doroshow JH, Poplin EA, Goodin S, Mauro D, Rubin EH. Pharmacokinetics of cetuximab after administration of escalating single dosing and weekly fixed dosing in patients with solid tumors. Clin Cancer Res. 2006; 12:6517–6522. [PubMed: 17065274]

25. Cao YG, Jusko WJ. Incorporating target-mediated drug disposition in a minimal physiologically-based pharmacokinetic model for monoclonal antibodies. J Pharmacokinet Pharmacodyn. 2014 in press.

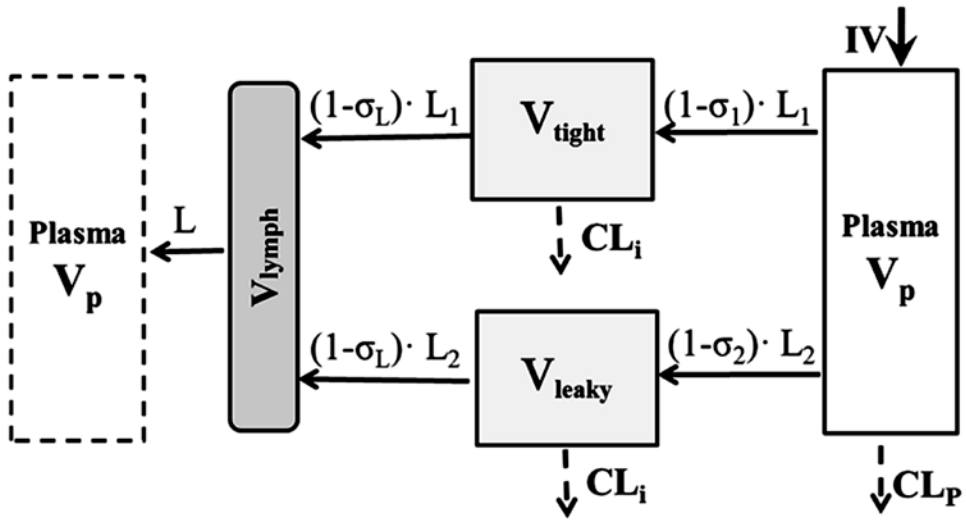

Figure 1.

Second-generation minimal PBPK model for monoclonal antibody pharmacokinetics. Symbols and physiological restrictions are defined in Eq (1) – (6). Clearance is applied either to plasma or interstitial fluid. The plasma compartment in the left box represents the venous plasma as in full PBPK models but is not applied in this model.

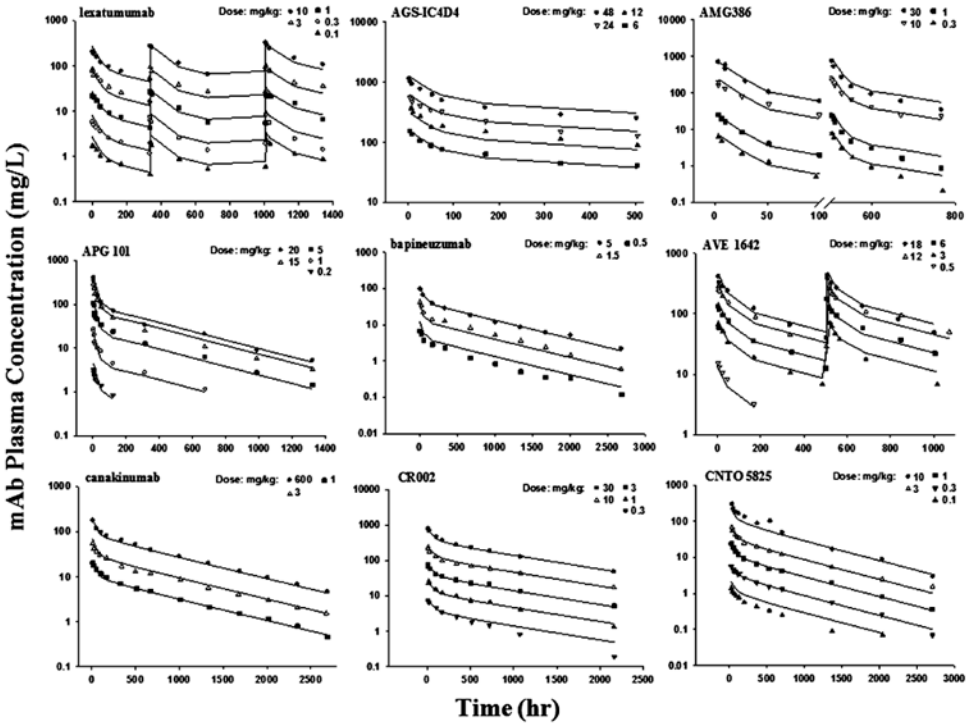

Figure 2.

Pharmacokinetic profiles of 9 monoclonal antibodies in human subjects. Symbols are observations and curves are mPBPK model fittings.

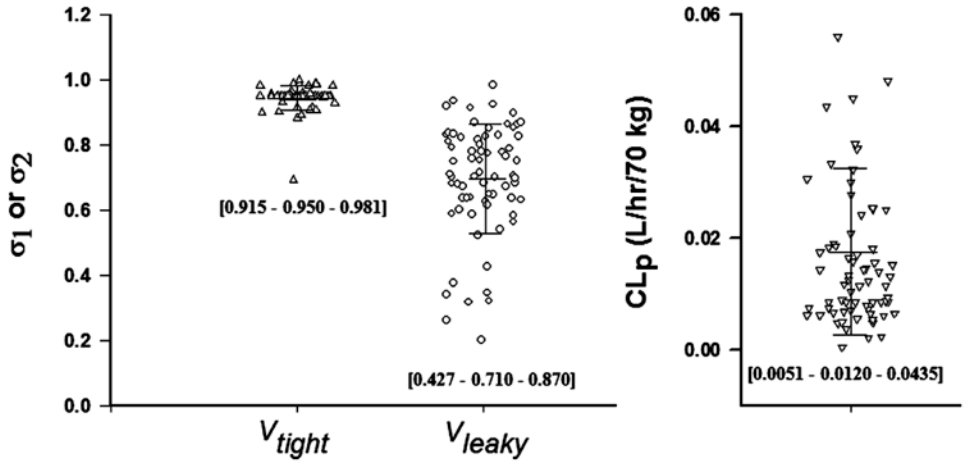

Figure 3.

The estimated parameters of 72 monoclonal antibodies using the second-generation minimal PBPK model for the reflection coefficients (σ_1 and σ_2) for two groups of tissues (V_{tight} and V_{leaky}) using the model when CL_p applies. Bars indicate mean and standard deviation. Numbers in brackets are [10% - 50% - 90%] percentiles.

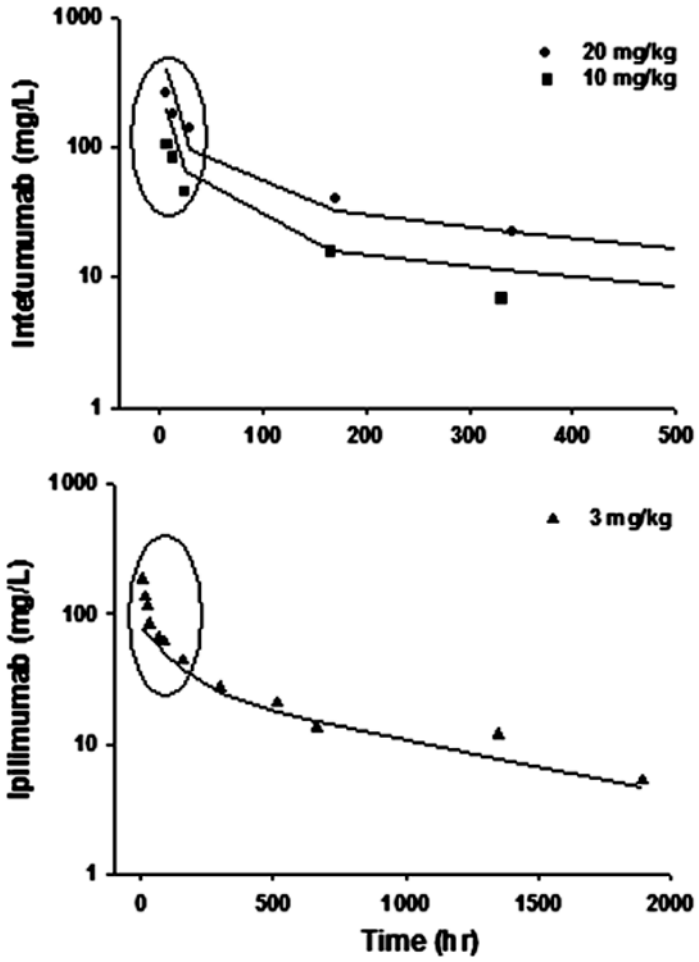

Figure 4.

Profiles of two representative monoclonal antibodies where the minimal PBPK model was suboptimal. The circles highlight the primary mis-fitted data points.

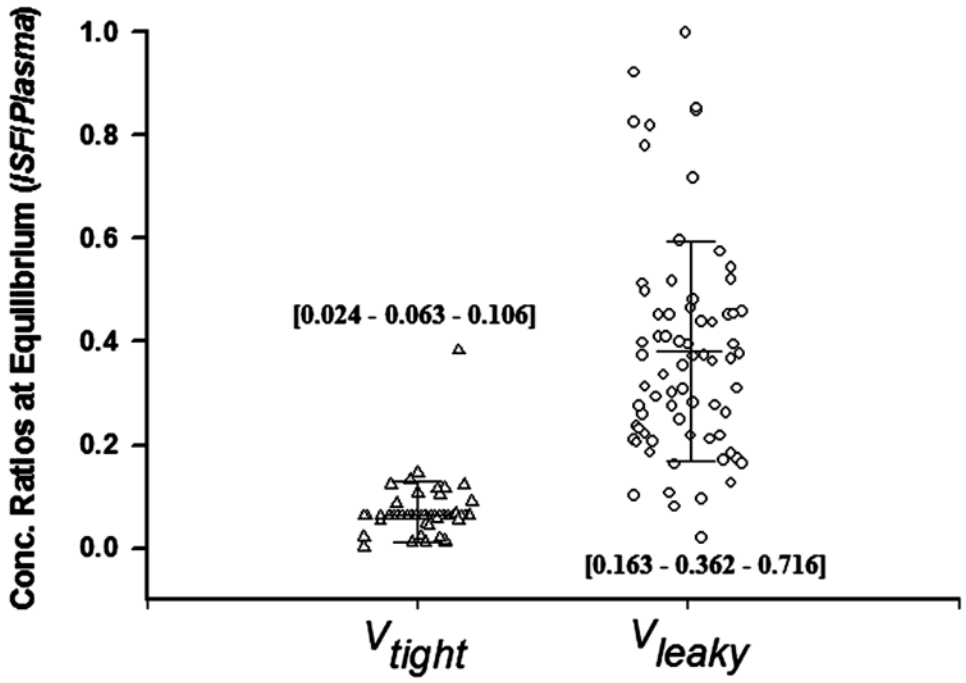

Figure 5.

Predicted mAb concentration ratios of interstitial fluid (*ISF*): plasma at equilibrium using the model with CL_p. Bars depict mean and standard deviation. Numbers in brackets are [10% - 50% - 90%] percentiles.

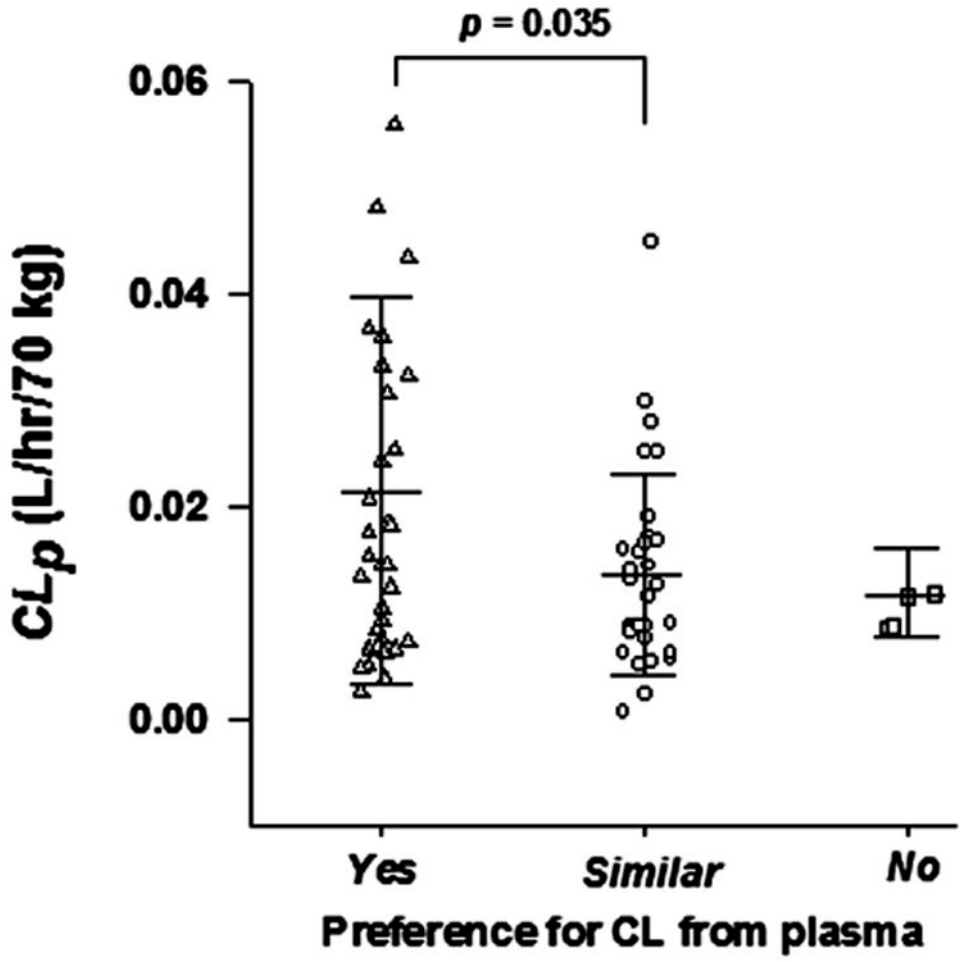

Figure 6.

The estimated plasma clearance (CL_p) of monoclonal antibodies in groups with "Yes" "Similar" and "No" preference for fittings with plasma clearance (CL_p). Three categories are defined in the text. The student t-test was applied.

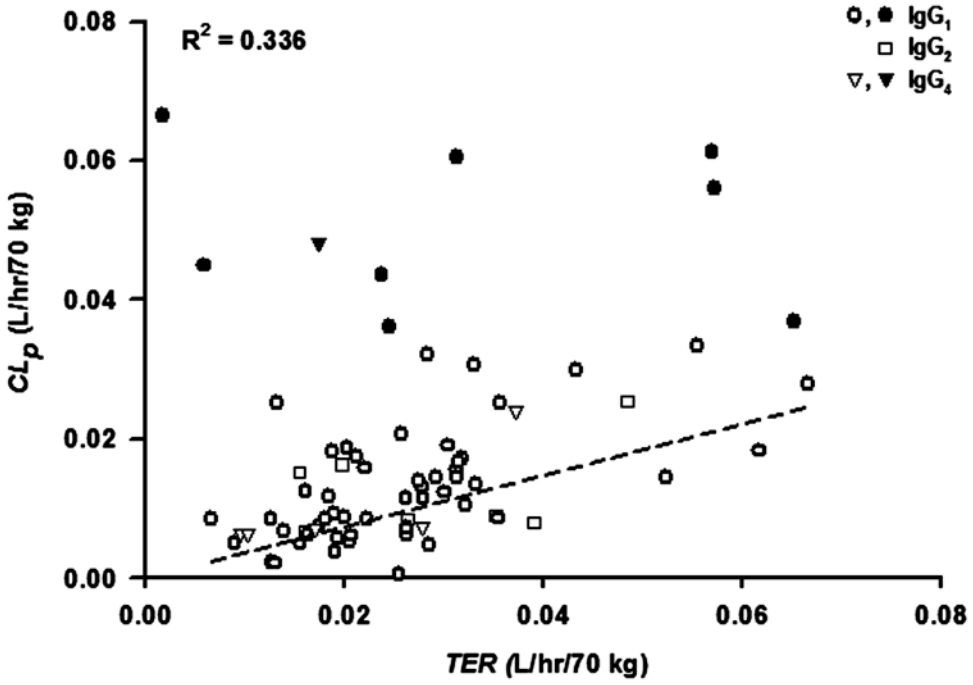

Figure 7.

Correlation between plasma clearance (CL_p) and Transcapillary Escape Rate (*TER*). The linear regression line (forced through (0,0); slope = 0.37) and correlation coefficient are shown for mAbs with CL_p < 0.035 L/hr/70 kg. Solid symbols: clearance > 0.035 L/hr/70 kg; open symbols: clearance < 0.035 L/hr/70 kg.

Table 1

Pharmacokinetic parameters of monoclonal antibodies (mAb) in man.

			Model with CL_p (L/hr/70 kg)				Model with CL_i (L/hr/70 kg)				
Name	**Type**	**Ref** [a]	σ_1	σ_2	CL_p	*Obj* [b]	σ_1	σ_2	CL_i	*Obj*	*Preference for* CL_p [c]
Adalimumab	IgG_1	[S1]	0.950[d]	0.628	0.0104	89.5	0.515	0.476	<0.0001	112.4	Yes
Adecatumumab	IgG_1	[S2]	0.883	0.524	0.0300	223.2	0.416	0.296	0.0318	220.8	Similar
Aflibercept	IgG_1	[S3-5]	0.950	0.340	0.0333	91.0	0.762	<0.001	0.0362	88.9	Yes
AGS-1C4D4	IgG_1	[S6]	0.950	0.701	0.0062	172.1	1.000	0.562	0.0176	171.6	Similar
Alefacept	IgG_1	[S7]	0.950	0.682	0.0131	-14.1	0.950	0.460	0.0268	-17.1	Similar
AMG102	IgG_2	[S8]	0.950	0.590	0.0090	109.0	0.950	0.438	0.0160	107.8	Similar
AMG386	IgG_1	[S9]	0.950	0.321	0.0612	204.1	<0.001	<0.001	0.0529	201.5	Yes
APG101	IgG_1	[S10]	0.950	0.202	0.0278	153.9	0.579	<0.001	0.0223	152.1	Similar
AS1402	IgG_1	[S11]	0.950	0.862	0.0251	115.3	0.950	0.471	0.0964	113.3	Similar
AVE1642	IgG_1	[S12]	0.950	0.639	0.0156	244.0	0.916	0.418	0.0285	242.2	Similar
Bapineuzumab	IgG_1	[S13]	0.950	0.587	0.0086	56.5	0.822	0.531	0.0134	56.4	Similar
Basiliximab	IgG_1	[S14,S15]	0.950	0.649	0.0191	45.3	0.896	0.320	0.0299	43.8	Similar
Belimumab	IgG_1	[S16]	0.958	0.759	0.0175	95.5	0.511	0.738	0.0351	92.8	Yes
Bevacizumab	IgG_1	[S17]	0.950	0.869	0.0086	256.8	0.990	0.683	0.0343	254.1	Similar
Canakinumab	IgG_1	[S18]	0.917	0.716	0.0073	66.5	0.870	0.577	0.0118	109.2	Yes
Cantuzumab mertansine	IgG_1	[S19]	0.990	0.984	0.0664	58.2	<0.001	0.483	0.2785	57.3	Yes
CαStx2	IgG_1	[S20]	0.950	0.775	0.0186	178.5	0.950	0.455	0.0417	170.1	No
CAT-354	IgG_4	[S21,S22]	0.928	0.919	0.0066	87.9	0.556	1.000	0.0201	91.7	Yes
CDP571	IgG_4	[S23]	0.950	0.811	0.0482	44.4	0.874	<0.001	0.0926	41.9	Yes
CGP 51901	IgG_1	[S24]	0.950	0.702	0.0115	82.3	0.950	0.522	0.0307	73.8	No
CNTO 5825	IgG_1	[S25]	0.902	0.832	0.0075	100.4	0.644	0.874	0.0182	100.5	Yes
Conatumumab	IgG_1	[S26,S27]	0.950	0.790	0.0038	87.2	0.774	0.854	0.0097	86.8	Yes
CR002	IgG_1	[S28]	0.907	0.854	0.0049	114.2	0.746	0.874	0.0141	114.1	Yes
Daclizumab	IgG_1	[S29,S30]	0.950	0.263	0.0183	59.1	0.913	< 0.001	0.0172	58.0	Yes

Name	Type	Ref [a]	Model with CL_p (L/hr/70 kg)				Model with CL_i (L/hr/70 kg)				*Preference for CL_p* [c]
			σ_1	σ_2	CL_p	*Obj* [b]	σ_1	σ_2	CL_i	*Obj*	
Drozitumab	IgG_1	[S31]	0.908	0.685	0.0146	107.1	0.614	0.627	0.0242	107.0	Yes
F105	IgG_1	[S32]	0.950	0.633	0.0171	69.5	0.950	0.285	0.0257	67.5	Similar
Galiximab	IgG_1	[S33,S34]	0.950	0.672	0.0048	338.4	0.749	0.878	0.0169	318.8	Yes
Ganitumab	IgG_1	[S35]	0.950	0.584	0.0252	329.4	0.630	0.364	0.0345	328.7	Similar
Gevokizumab	IgG_2	[S36]	0.931	0.837	0.0067	-20.1	0.757	0.834	0.0193	-20.0	Yes
GNbAC1	IgG_4	[S37]	0.915	0.831	0.0071	56.1	0.776	0.787	0.0189	53.9	Yes
Golimumab	IgG_1	[S38,S39]	0.950	0.793	0.0182	43.1	0.950	0.489	0.0457	52.8	Yes
Hu12F6mu	IgG_2	[S40]	0.950	0.427	0.0254	-16.2	0.929	< 0.001	0.0276	-18.5	Yes
Infliximab	IgG_1	[S41]	0.990	0.924	0.0085	127.9	0.738	0.954	0.0572	127.9	Yes
KB001	Fab’	[S42]	0.950	0.753	0.0158	42.4	0.756	0.617	0.0355	42.1	Similar
Lexatumumab	IgG_1	[S43]	0.950	0.685	0.0140	216.8	0.950	0.445	0.0283	213.7	Similar
Lumiliximab	IgG_1	[S44]	0.962	0.780	0.0057	66.7	0.950	0.692	0.0125	64.8	Similar
Gemtuzumab ozogamicin	IgG_1	[S45]	0.950	0.638	0.0605	-7.4	0.283	< 0.001	0.0831	-12.7	Yes
MDX-1106	IgG_1	[S46]	0.950	0.899	0.0065	73.4	0.551	0.966	0.0150	78.4	Yes
MEDI-528	IgG_4	[S47]	0.987	0.754	0.0054	113.4	0.942	0.735	0.0182	112.5	Similar
MEDI-563	IgG_1	[S48]	0.950	0.826	0.0125	19.4	0.950	0.600	0.0334	18.1	Similar
Mepolizumab	IgG_1	[S49]	0.950	0.750	0.0085	64.5	0.950	0.591	0.0193	58.2	No
MGAWN1	IgG_1	[S50]	0.950	0.915	0.0051	160.5	0.950	0.799	0.0226	161.5	Similar
Mogamulizumab	IgG_1	[S51]	0.950	0.378	0.0144	69.2	0.894	0.156	0.0157	68.7	Yes
Natalizumab	IgG_4	[S52]	0.950	0.565	0.0242	37.1	0.950	0.017	0.0287	35.9	Yes
Obinutuzumab	IgG_1	[S53]	0.946	0.870	0.0024	642.0	0.873	0.880	0.0095	642.0	Yes
Ocrelizumab	IgG_1	[S54]	0.950	0.706	0.0208	71.9	0.501	0.631	0.0345	71.4	Yes
Pagibaximab	IgG_1	[S55]	0.950	0.864	0.0022	34.1	0.950	0.826	0.0109	33.6	Similar
PAmAb	IgG_1	[S56]	0.950	0.779	0.0087	184.4	0.950	0.621	0.0224	180.2	No
Panobacumab	IgM	[S57]	0.950	0.732	0.0435	172.7	0.952	0.000	0.0729	164.0	Yes
Pateclizumab	IgG_1	[S58]	0.950	0.638	0.0144	76.7	0.848	0.441	0.0231	76.1	Similar
PRO95780	IgG_1	[S59]	0.984	0.638	0.0124	107.7	0.575	0.702	0.0189	107.8	Yes

J Pharmacokinet Pharmacodyn. Author manuscript; available in PMC 2015 December 01.

J Pharmacokinet Pharmacodyn. Author manuscript; available in PMC 2015 December 01.

Name	Type	Ref [a]	Model with CL_p (L/hr/70 kg)				Model with CL_i (L/hr/70 kg)				*Preference for CL_p* [c]
			σ_1	σ_2	CL_p	*Obj* [b]	σ_1	σ_2	CL_i	*Obj*	
Rilotumumab	IgG_2	[S60]	0.950	0.699	0.0085	168.9	0.950	0.553	0.0194	167.5	Similar
Rituximab	IgG_1	[S54]	0.894	0.826	0.0118	73.2	0.680	0.644	0.0199	69.1	No
Siltuximab	IgG_1	[S61]	0.965	0.673	0.0115	281.0	0.950	0.467	0.0218	279.8	Similar
Siplizumab	IgG_1	[S62]	0.950	0.318	0.0560	4.8	0.770	<0.001	0.1669	-0.7	Yes
Solanezuma	IgG_1	[S63]	0.950	0.852	0.0068	98.2	0.950	0.666	0.0150	104.1	Yes
TB-402	IgG_4	[S64]	0.950	0.681	0.0074	50.9	0.950	0.552	0.0154	49.9	Similar
Tefibazumab	IgG_1	[S65]	0.902	0.815	0.0093	102.0	0.644	0.819	0.0215	100.2	Yes
Tigatuzumab	IgG_1	[S66]	0.950	0.710	0.0005	108.0	0.876	0.749	0.0008	108.0	Similar
Tremelimumab	IgG_2	[S67]	0.954	0.541	0.0080	108.2	0.890	0.443	0.0116	107.2	Similar
Urtoxazumab	IgG_1	[S68]	0.957	0.766	0.0062	28.2	0.865	0.720	0.0157	27.5	Similar
Vedolizumab	IgG_1	[S69]	0.950	0.823	0.0062	281.3	0.950	0.701	0.0185	290.2	Yes
Visilizumab	IgG_2	[S70]	0.949	0.834	0.0152	-35.2	0.567	0.806	0.0390	-34.6	Yes
HGS004	IgG_1	[S71]	0.983	0.601	0.0306	90.9	0.874	0.149	0.0433	93.4	Yes
HuMV833	IgG_1	[S72]	0.981	0.936	0.0449	68.6	0.950	0.400	very high	69.3	Similar
KBPA-101	IgG_1	[S73]	0.990	0.703	0.0361	88.9	0.950	0.125	0.0700	86.4	Yes
R1507	IgG_1	[S74]	0.950	0.615	0.0134	74.2	0.950	0.377	0.0001	77.1	Yes
Trastuzumab	IgG_1	[S75]	0.950	0.636	0.0168	127.6	0.950	0.380	0.0335	126.3	Similar
Tocilizumab	IgG_1	[S76]	0.693	0.346	0.0368	96.8	0.215	0.048	0.0287	96.8	Yes
Raxibacumab	IgG_1	[S77]	0.950	0.802	0.0085	173.9	0.950	0.648	0.0241	171.2	Similar
Panitumumab	IgG_2	[S78]	0.950	0.781	0.0164	67.4	0.950	0.509	0.0461	66.5	Similar
Cetuximab	IgG_1	[S79]	0.999	0.650	0.0322	106.0	0.950	0.154	0.0560	104.0	Yes

[a] References provided in Supplementary Materials.

[b] Value of objective function in ADAPT-V.

[c] Three categories are defined in text.

[d] 0.95 for $\sigma 1$ was a fixed value.

Table 2

Monoclonal antibodies that failed in model application.

Antibodies	Type	Ref [a]	Fittings or estimated parameters	Speculative reasons
Afelimomab	$(Fab)_2$	[S80]	over-prediction of initial phase, tiny σ_1 and σ_2	nonspecific binding in blood
AHM	IgG_1	[S81]	over-prediction of initial phase, tiny σ_1 and σ_2	nonspecific binding in blood
Bavituximab	IgG_1	[S82]	over-prediction of initial phase, tiny σ_1 and σ_2	nonspecific binding in blood
Intetumumab	IgG_1	[S83]	over-prediction of initial phase, tiny σ_1 and σ_2	nonspecific binding in blood
Roledumab	IgG_1	[S84]	over-prediction of initial phase, tiny σ_1 and σ_2	nonspecific binding in blood
SB 249417	IgG_1	[S85]	over-prediction of initial phase, tiny σ_1 and σ_2	nonspecific binding in blood
Anti-IL-12p40	IgG_1	[S86]	$\sigma_1 < \sigma_2$ for both clearance mechanisms	unknown
Ipilimumab	IgG_1	[S87]	under-prediction of initial phase	measurement error
MDX-1303	IgG_1	[S88]	under-prediction of initial phase	measurement error
Ponezumab	IgG_2	[S89]	under-prediction of initial phase	measurement error
Sirukumab	IgG_1	[S90]	$\sigma_1 < \sigma_2$ for both clearance mechanisms	unknown

[a] References provided in Supplementary Materials